

The correlation histopathological and conventional/advanced MRI techniques in glial tumors

La correlación histopatológica y la resonancia magnética convencionales/avanzadas en tumores gliales

Selim Seker¹, Tamer Altay², Ece Uysal², Hidayet S. Cine^{3*}, Ahmed Y. Yavuz², and Idris Avci⁴

¹Department of Neurosurgery, Istinye University, Liv Hospital; ²Department of Neurosurgery, University of Health Sciences, Prof. Dr. Cemil Tascioglu City Hospital; ³Department of Neurosurgery, Istanbul Medeniyet University, Prof. Dr. Suleyman Yalcin City Hospital; ⁴Department of Neurosurgery, Spinal Health Center, Memorial Hospital. Istanbul, Turkey

Abstract

Objective: We aimed to elucidate the histopathological pre-diagnosis of cranial gliomas with magnetic resonance imaging (MRI) techniques in gliomas. **Method:** A total of 82 glioma patients were enrolled to our study. Pre-operative conventional MRI images (non-contrast T1/T2/flair/contrast-enhanced T1) and advanced MRI images (DAG and ADC mapping, MRI spectroscopy and perfusion MRI [PMRI]) were analyzed. **Results:** Conventional MRI alone is useful in radiological pre-evaluation in low-grade glioma in 54.8% and 86.3% in high-grade glioma. Additional advanced MRI techniques were beneficial in comparing low-grade gliomas in 98% and 83.9% in high-grade glioma. On ROC analysis, ADC cutoff value 0.905 mm²/s ($p = 0.001$), rCBV cutoff value 1.77 ($p = 0.001$), Cho/NAA cut-off value 2.20 ($p = 0.001$), and Cho/Cr cutoff value 2.01 ($p = 0.001$) were achieved. Significant results were obtained when ADC, Cho/NAA, and Cho/Cr were analyzed into four histopathologically grade groups besides ($p = 0.001$). NAA/Cr values were not significant in pathological grading. rCBV measurements were statistically significant between Grades I and IV and between II and IV. **Conclusion:** Using additional advanced MRI techniques such as PMRI, magnetic resonance spectroscopy, and DWI with conventional MRI could enhance the accuracy of histopathological grading in cranial glioma.

Keywords: Glioma. MR spectroscopy. Perfusion MRI. Diffusion-weighted MRI. Histopathological grading.

Resumen

Objetivo: Nos propusimos dilucidar el pre-diagnóstico histopatológico de los gliomas craneales con técnicas de resonancia magnética en gliomas. **Método:** Un total de 82 pacientes con glioma fueron incluidos en nuestro estudio. Se analizaron imágenes pre-operatorias de RM convencional (T1/T2/flair/contraste realizado T1) e imágenes de RM avanzada (mapeo DAG y ADC, espectroscopia de RM y RM de perfusión). **Resultados:** Las técnicas avanzadas adicionales de RM fueron beneficiosas en la comparación de los gliomas de bajo grado en el 98% y en el 83,9% en el glioma de alto grado. En el análisis ROC se alcanzó un valor de corte ADC de 0,905 mm²/s ($p = 0,001$), un valor de corte rCBV de 1,77 ($p = 0,001$), un valor de corte Cho/NAA de 2,20 ($p = 0,001$) y un valor de corte Cho/Cr de 2,01 ($p = 0,001$). Se obtuvieron resultados significativos cuando se analizaron ADC, Cho/NAA y Cho/Cr en cuatro grupos de grado histopatológico además ($p = 0,001$). Los valores de NAA/Cr no fueron significativos en la gradación patológica. Las mediciones de rCBV fueron estadísticamente significativas entre los grados I y IV y entre II y IV. **Conclusión:** El uso de técnicas avanzadas adicionales de RM como la RMMP, la ERM y la DWI junto con la RM convencional podría mejorar la precisión de la gradación histopatológica en el glioma craneal.

Palabras clave: Glioma. Espectroscopia de RM. RM de perfusión. RM ponderada en difusión. Graduación histopatológica.

*Correspondence:

Hidayet S. Cine

E-mail: cinesafak@gmail.com

Date of reception: 27-12-2023

Date of acceptance: 13-02-2024

DOI: 10.24875/CIRU.23000648

Cir Cir. (ahead of print)

Contents available at PubMed

www.cirugiaycirujanos.com

0009-7411/© 2024 Academia Mexicana de Cirugía. Published by Permanyer. This is an open access article under the terms of the CC BY-NC-ND license (<http://creativecommons.org/licenses/by-nc-nd/4.0/>).

Introduction

Imaging methods in gliomas are aimed at pre-operative diagnosis, determining tumor grade and prognosis, radiotherapy and surgical planning, and guiding treatment. The most commonly used imaging method is contrast-enhanced magnetic resonance imaging (MRI). Conventional MRI plays a primary role in evaluating tumor localization, heterogeneity, vascularization, contrast enhancement, peri-tumoral edema, and proximity to important anatomical-functional centers. Secondary tumor findings such as cystic formations, calcification (oligodendroglioma), necrosis (glioblastoma), and hemorrhage (high-grade glioma) are guiding in the differential diagnosis^{1,2}. The World Health Organization (WHO) classification is inadequate in important issues such as the anatomical localization of the tumor, its size, degree of surgical accessibility or resectability, biological behavior, and prediction of response to treatment. Similarly, conventional MRI is limited in predicting these criteria. For this reason, the use of various functional MRI methods is preferred to determine the tumor degree³.

Magnetic resonance spectroscopy (MRS) is a non-invasive functional MRI method that provides biochemical and metabolic information about the tissue. The most important differential diagnosis in this neuroimaging is the distinction between neoplastic-non-neoplastic or low-high-grade tumors⁴. Perfusion MRI (PMRI) is a non-invasive functional MRI method that provides information about tissue blood flow, *in vivo* tumor angiogenesis, and tumor microcirculation at the microscopic level. Increased vascularity corresponds to increased tumor stage and maximum cerebral blood volume (CBV)⁵.

Gliomas are the most common brain neoplasm in adults and a major cause of mortality and morbidity. According to the revised WHO classification, central nervous system tumors are grouped based on microscopic imaging. In this classification, neuroepithelial tumors are divided into astrocytic neoplasms, oligodendroglial, oligoastrocytic, ependymal, and choroid plexus tumors. The tumor stage indicates the degree of malignancy and is closely related to survival and prognosis. Staging of gliomas is performed by taking into account histopathologically the presence of mitotic activity, necrosis, and infiltration, which indicate uncontrolled growth and the vascularity of the tumor. The tumor is graded from Grade I to Grade IV: I–II is considered low grade, and III–IV is regarded as high

grade. Increased cellularity, atypic cells, and an increase in mitotic activity, endothelial hyperplasia, necrosis, and angiogenesis are additionally observed in Grade IV glioblastomas⁶.

In recent years, MRI has changed from the morphological imaging of the tissue to the functional, metabolic, cellular characterization, and secondary biological behavior of the tumor, and to predict the diagnosis, grade, response to treatment, and prognosis with advanced imaging methods. The MRI sequences, including non-contrast T1, T2, FLAIR, contrast-enhanced T1, MRS, PMRI, and diffusion MRI, were performed. Choline (Cho)/N-acetyl aspartate (NAA), NAA/Creatine (Cr), and Cho/Cr ratios, as well as lipid and lactate levels, are utilized as markers, especially useful in the diagnosis of tumoral lesions but provide limited insight into the malignancy level of the tumor⁷.

Within the scope of this research, we aimed to elucidate the histopathological pre-diagnosis of cranial gliomas with conventional and advanced MRI techniques (DWI, PMRI, MRS, and ADC values) and investigate the integration of these visual tools in high and low-grade gliomas.

Method

In this research, patients who underwent MRI with the preliminary diagnosis of an intracranial mass were scanned backward from the picture archiving and communication system, and 82 cases with glial tumors between the ages of 15–94 were retrospectively analyzed. Conventional MRI findings, contrast enhancement features, DWI, MRS, PMRI findings, and ADC values were compared with pathology results. All procedures followed were in accordance with the ethical standards of the responsible committee on human experimentation (institutional and national) and with the Helsinki Declaration of 1975, as revised in 2008. Ethics committee approval was granted from our institution on 27/08/2019 with protocol number 48670771-514.10, and informed consent has been obtained from all participants.

MRI, MRS, PMRI, and ADC measurements

Conventional brain MRI, diffusion, MRS, and PMRI examinations were performed using a 1.5 Tesla MRI device (Magnetom Aera, Siemens, Erlangen, Germany) and a brain coil. The standard brain MRI protocol includes T1-weighted imaging with TR=426 ms, TE=99 ms, and slice thickness of 5 mm; T2-weighted imaging with TR = 4350 ms, TE = 102 ms, and slice thickness of

5 mm. In FLAIR sequences, TR = 9000 ms, TE = 86 ms, and slice thickness of 5 mm. For SWI imaging, TR = 49 ms and TE = 40 ms. Contrast-enhanced examinations were performed using 0.5 mmol/ml gadoteric acid. In contrast-enhanced T1-weighted imaging, TR is 402 ms and TE is 5.6 ms.

DWI was taken as TR = 4500 msec, TE = 98 msec, and section thickness as 5 mm. The diffusion-weighted sequence in the axial plane with single-shot echo-planar imaging by applying diffusion-sensitive gradients at three different b values ($b = 50$, $b = 400$, and $b = 800 \text{ mm}^2/\text{s}$) in all three directions (x, y, and z-axis). The device automatically creates ADC maps of isotropic images, and the average ADC values of all lesions were measured manually on these maps. Measurements of the lesions were made as follows: three circular ROIs (Region of Interest) were placed on the ADC map in the axial plane and measurements were made, and the arithmetic average of these measurements was taken. The ROI volume was kept at approximately 15-20 mm^2 .

MRS was used for spectroscopic examination using the PRESS (point-resolved spectroscopy) technique. Depending on the size and nature of the mass, a single-voxel or multi-voxel area of 8 cm^3 ($2 \times 2 \times 2 \text{ cm}$) was placed on the intracranial mass. To determine the volume to be selected for examination (volume of interest), axial, coronal, and sagittal images of the mass were obtained using the T2A sequence in the patient's cranial MRI. The spectroscopic voxels taken for examination were made so that the mass remained as far away from the vascular structures and edges of the mass as possible to prevent contamination of the surrounding tissues, and the voxel areas were checked in all three planes. For single-voxel MRS, TE = 135 msec, TR = 2000 msec; For multivoxel MRS, signals from NAA, choline, and creatinine protons were collected within the mass using the parameters TE = 135 msec, TR = 1700 msec. After the spectral data were obtained, the Cho/NAA, Cho/Cr, and NAA/Cr ratios of the masses were obtained using the major peak amplitudes of NAA, Cho, and Cr molecules.

rCBV values were obtained from PMRI as follows: 0.2 mmol/kg Gadoteric acid was administered through an automatic injector, followed immediately by 100 mL isotonic NaCl at a rate of 5 mL/s. Six times in an average of 90 s, consecutive images, each consisting of 20 images, were taken. Spin-echo echo-planar imaging sequences were used in the images taken. The resulting images were transferred to the workstation for post-processing. rCBV maps were obtained with ready-made software programs in the MRI system. When placing the ROI, cystic and non-necrotic areas of the mass and

adjacent vascular structures were avoided. The ROI volume was kept at approximately 5-8 mm^3 . 3 ROIs were placed on the lesions, and the arithmetic mean of the highest rCBV value was selected. The highest ROI obtained was compared with the white matter in the opposite hemisphere. Relative CBV ratio = $\text{rCBV (tumor)}/\text{rCBV (normal)}$ was obtained.

Evaluation

While evaluating intracranial masses, radiological findings were reviewed by an experienced radiologist in the following order: lesions were assessed as low and high grade by looking at the features of edema, cyst, hemorrhage, necrosis, and contrast enhancement among conventional MRI findings. Then, considering the predictive values obtained from studies that added diffusion, MRS, and perfusion examination findings from advanced MR imaging methods to conventional MRI were evaluated as low and high grades. Measurements were performed using diffusion, spectroscopy, and perfusion examination, which are advanced MRI examination methods. In the data obtained from the measurements, the importance of ADC, Cho/Cr, Cho/NAA, and rCBV ratios in both low and high-grade discrimination and pathological grading of the lesions was evaluated. All radiological ratings obtained were compared with the pathological results.

Statistical analysis

Patient data collected within the scope of the study were analyzed with the IBM Statistical Package for the Social Sciences (SPSS) for Windows 26.0 (IBM Corp., Armonk, NY) package program. Frequency and percentage for categorical data and mean and standard deviation for continuous data were given as descriptive values. For comparisons between groups, the "Independent Sample T-test" was used for two groups, and the "Pearson Chi-square test" was used to compare categorical variables. The results were considered statistically significant when the p-value was less than 0.05. ROC analysis for ADC measurements and rCBV ratios in distinguishing low- and high-grade glial tumors.

Results

The presence of edema, hemorrhage, necrosis, cystic focus content, and contrast enhancement characteristics in the lesions were assessed through

conventional MRI (Table 1). The results were as follows: edema was detected in 76.8%. When the lesions were examined to determine whether they contained a cystic component, cysts were observed in 50%, hemorrhagic focus and necrosis were detected in 54.9%, and hemorrhage in 45.1%. Additionally, 53.7% of the lesions had no necrosis. A majority of the lesions (84.1%) were contrasted to varying degrees. When the lesions were grouped as low and high grade according to conventional MRI findings, it was seen that 40.2% of the cases were low grade and 59.8% were high grade. The radiological grading based on conventional MRI findings was compatible with the pathological grading. However, the success rate of conventional MRI in detecting low-grade tumors was 54.8%, but high-grade tumors were higher at 86.3% (Fig. 1).

Radiological grading was performed by adding DWI and ADC maps, spectroscopy examination, and PMRI findings. In advanced MRI, the following was taken into consideration: the cutoff point in terms of ADC measurements in distinguishing low and high-grade lesions was $1.1 \times 10^{-3} \text{ mm}^2/\text{s}$ based on studies on the subject, NAA 2.0-2.02 ppm, Cho 3.22 ppm from spectroscopic measurements. The cutoff point for the rCBV ratio was 1.75 from perfusion

MRI findings, with a range of 3.0-3.02 ppm, Cho/NAA ratio between 2-2.5, and Cho/Cr ratio between 2-2.5. The radiological grading was compatible with the pathological results. However, the success of the combination of conventional and advanced MRI in detecting low-grade tumors (83.9%) was better than the grading performed with conventional MRI alone. The detection rate for high-grade tumors was higher (98%) (Table 2).

On ROC analysis, the ADC cutoff value was $0.905 \text{ mm}^2/\text{s}$ ($p = 0.001$), rCBV cutoff value 1.77 ($p = 0.001$), Cho/NAA cutoff value 2.20 ($p = 0.001$), and Cho/Cr cutoff value 2.01 ($p = 0.001$) with statistical significance. Significant results were obtained when ADC, Cho/NAA, and Cho/Cr were analyzed into four histopathologically grade groups besides Grade III and IV ($p = 0.001$). NAA/Cr values were insignificant in pathological grading ($p > 0.05$).

ROC analysis was performed with rCBV ratios measured in discriminating low and high-grade lesions. The size of the area under the curve was 0.920, and this was statistically significant ($p = 0.001$). The cutoff value for rCBV ratios was 1.77. The sensitivity value was 94.1%, and the specificity value was 64.5% (Fig. 2).

The rCBV ratios were added to the PMRI findings and the conventional MRI, and the cutoff point for the rCBV ratio was taken as 1.77. The radiological grading

Table 1. Results of conventional radiological characteristics

Demographics	Low-grade	High-grade	p-value
	n (%)		
Gender	16 (51%)	33 (64%)	
Male	15 (48%)	18 (35%)	
Female			
Tumor grade			
Pathological	31	51	0.189
Conventional MRI	33	49	0.020*
Contrast enhancement	67.70%	94.10%	0.001*
Necrosis	12.90%	66.70%	0.001*
Hemorrhage	12.90%	64.70%	0.325
Cyst	45.20%	52.90%	0.001*
Edema	45.20%	96.10%	0.289
con + adv MRI	83.90%	98%	

*p < 0.05: statistical significance.

con: conventional; adv: advanced; MRI: magnetic resonance imaging.

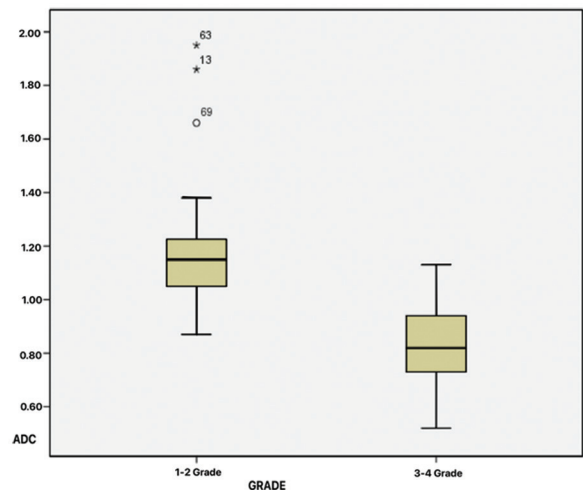


Figure 1. Comparison of grading according to conventional magnetic resource imaging and ADC association findings with pathological grading.

was compatible with the pathological results. However, the success rate of the combination of conventional MRI and rCBV findings in detecting low-grade tumors was 74.2%, and the rate of detecting high-grade tumors was higher at 92.2%.

Diffusion MRI and ADC maps were added to conventional MRI findings, and the cutoff point for ADC was taken as $0.905 \times 10^{-3} \text{ mm}^2/\text{s}$. The radiological grading was compatible with the pathological results. However, while the success rate of combining conventional MRI and ADC findings in detecting low-grade tumors was 64.5%, the rate of detecting high-grade tumors was 73.2%.

Table 2. Comparison of ADC, Cho/NAA, Cho/Cr, NAA/Cr, and NAA/Cr values in distinguishing low- and high-grade lesions

MRI	Grade of tumor	n (%)	Median ± SD (minimum-maximum)	p-value
ADC	Low	31 (37%)	1.12 ± 0.24 (0.87-1.95)	0.001*
	High	51 (62%)	0.83 ± 0.16 (0.52-1.95)	
Cho/NAA	Low	31 (37%)	3.51 ± 2.70 (0.59-9.60)	0.004*
	High	51 (62%)	5.73 ± 4.06 (0.29-19.53)	
Cho/Cr	Low	31 (37%)	1.97 ± 1.10 (0.52-4.60)	0.001*
	High	51 (62%)	3.99 ± 4.13 (0.63-19.70)	
NAA/Cr	Low	31 (37%)	0.77 ± 0.45 (0.00-1.58)	525
	High	51 (62%)	0.83 ± 0.86 (0.15-4.90)	
rCBV ratio	Low	31 (37%)	1.64 ± 0.72 (0.95-3.58)	0.001*
	High	51 (62%)	3.76 ± 1.66 (1.04-11.22)	

*p < 0.05: statistical significance.

SD: standard deviation; MRI: magnetic resonance imaging; ADC: apparent diffusion coefficient; Cho/NAA: Cholin/N-Asetilaspartat; Cho/Cr: Cholin/Creatin; NAA/Cr: N-asetilaspartat/creatin; rCBV: regional cerebral blood volume.

Radiological grading was performed again by adding the cutoff points obtained from advanced MRI examinations such as DWI and ADC maps, spectroscopy examination, and PMRI examination to the conventional MRI findings. When the new rating made using the cutoff points, we obtained was compared with the pathological rating, it was seen that the radiological rating was compatible with the pathological rating. However, the success rate of the combination of conventional and advanced MRI in detecting low-grade tumors was 77.4%. The detection rate for high-grade tumors was higher, 98% (Table 3 and Fig. 3).

On ROC analysis, ADC cutoff value 0,905 mm²/s (p = 0.001), rCBV cutoff value 1.77 (p = 0.001), Cho/NAA cutoff value 2.20 (p = 0,001), and Cho/Cr cut-off value 2.01 (p = 0.001) were achieved. Significant results were obtained when ADC, Cho/NAA, and Cho/Cr were analyzed into four histopathologically grade groups besides (p = 0.001). NAA/Cr values were not significant in pathological grading. rCBV measurements were statistically significant between Grades I and IV and between II and IV.

Discussion

In recent years, MRI sequences have been developed that allow us to obtain accurate information

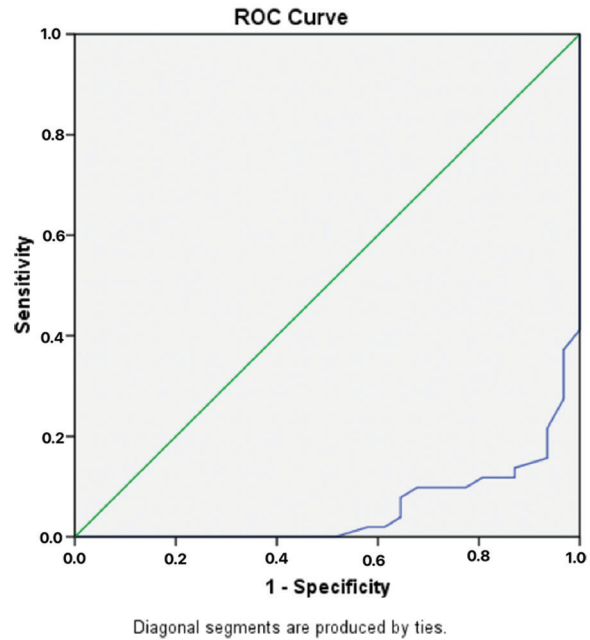


Figure 2. ROC analysis for ADC measurements in distinguishing low- and high-grade glial tumors.

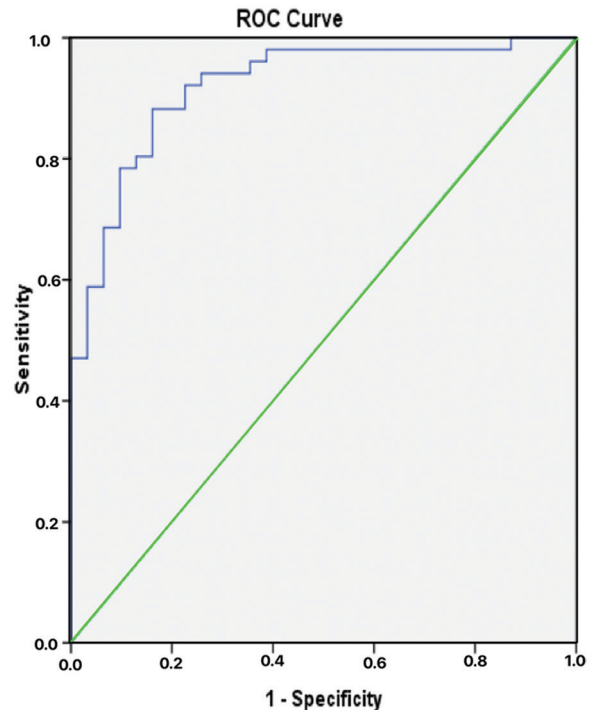


Figure 3. ROC analysis for rCBV ratios in differentiating low- and high-grade glial tumors.

about tumor physiology and anatomical information about brain tumors, and these are called “Advanced MR Imaging Methods.” Advanced MR imaging

Table 3. Comparison of ADC, Cho/NAA, Cho/Cr, NAA/Cr, and NAA/Cr values in distinguishing low and high-grade lesions in advanced MRI

MRI	Grade	n	Median ± SD (minimum-maximum)	p-value
ADC	1	4	1.55 ± 0.33 (1.19-1.95)	KW = 48.41 0.001*
	2	27	1.15 ± 0.18 (0.87-1.86)	
	3	17	0.88 ± 0.16 (0.62-1.13)	
	4	34	0.80 ± 0.15 (0.52-1.09)	
Cho/NAA	1	4	1.68 ± 1.91 (0.59-4.55)	KW = 11.54 0.009*
	2	27	3.78 ± 2.72 (0.80-9.60)	
	3	17	6.31 ± 3.80 (1.86-13.00)	
	4	34	6.45 ± 4.21 (0.29-19.53)	
Cho/Cr	1	4	1.22 ± 0.46 (0.62-1.74)	KW = 14.39 0.002*
	2	27	2.08 ± 1.13 (0.52-4.60)	
	3	17	3.56 ± 1.46 (1.10-6.00)	
	4	34	4.21 ± 4.96 (0.63-19.70)	
NAA/Cr	1	4	1.14 ± 0.56 (0.38-1.58)	KW = 2.62 0.453
	2	27	0.71 ± 0.42 (0.00-1.57)	
	3	17	0.74 ± 0.57 (0.20-2.03)	
	4	34	0.88 ± 0.98 (0.15-4.90)	
rCBV ratio	1	4	1.88 ± 0.78 (1.15-2.97)	KW = 40.61 0.001*
	2	27	1.61 ± 0.71 (0.95-3.58)	
	3	17	3.61 ± 1.53 (1.04-7.44)	
	4	34	3.83 ± 1.74 (1.64-11.22)	

*p < 0.05: statistical significance.

SD: standard deviation; MRI: magnetic resonance imaging; ADC: apparent diffusion coefficient; Cho/NAA: Cholin/N-Asetilspartat; Cho/Cr: Cholin/Creatin; NAA/Cr: N-Asetilspartat/Creatin; rCBV: regional cerebral blood volume; KW: Kruskal-Wallis.

methods allow numerically measuring dynamic physiological processes in the brain and providing qualitative information about tissue physiology. Using this qualitative data, the biological behavior of the tumor, the patient's life expectancy, and treatment processes can be predicted before the operation⁶⁻⁸. According to the results of our study, MRI techniques have been shown to be useful in grading glial tumors with proper and accurate use of MRI techniques to make pathological diagnoses in advance.

While conventional MRI plays a vital role in determining the localization of intracranial masses, their relationship with critical anatomical structures, and especially the treatment approaches, it can also give us insight into the grading of gliomas^{6,7}.

Law et al. reported the rate of determining the degree of high-grade gliomas with conventional MRI was 72.5%⁹, whereas Arvinda et al. stated 72.7%¹⁰. In our study, the conventional MRI findings in detecting low-grade glial tumors were 54.8%; the success rate in detecting high-grade glial tumors was 86.3%, and these results were compatible with the literature.

However, determining the degree of gliomas using conventional MRI has been limited. Moller-Hartmann et al. published that their reliability was between 55.1% and 83.3%¹¹. Gene Kondziolka et al. demonstrated a 50% false-positive rate in evaluating supratentorial gliomas¹². In another study, Lee et al. found that 50% of patients with low-grade astrocytoma detected on conventional MR imaging had high-grade astrocytoma on histopathological examination¹³.

In our study, conventional MRI findings such as edema, hemorrhage, necrosis, and contrast enhancement significantly distinguished low and high-grade lesions according to pathological outcomes. A cyst in the lesion was observed in 45.2% of the low-grade lesions and 52.9% of the high-grade lesions.

The contrast enhancement in conventional MRI has an important place in tumor grading in glial tumors, but it is not significant alone in tumor grading. Barker et al. investigated the histopathology results of 31 patients without contrast enhancement, and they found that 32% were Grade III and 4% were Grade IV¹⁴. In another study, Fan et al. stated that 14% of non-enhancing supratentorial gliomas were high-grade¹⁵. Dean et al. indicated that the mass effect and necrosis were two crucial determinants of tumor grade. However, they also noted that a high-grade glioma may be confused with a low-grade glioma when it does not have sufficient edema, contrast medium enhancement, necrosis, and mass effect¹⁶. Considering all these studies and the results of our study, due to the heterogeneous internal structure of tumors and the inability of conventional MRI to provide detailed information about tumor physiology and metabolites, the correlation of traditional MRI with tumor histopathology remains limited.

Conventional MR imaging with gadolinium-based contrast agents is an accepted tool for characterizing brain tumors. However, DWI, perfusion-weighted imaging, and MRS are relatively newer techniques that provide additional microstructural, microvascular, and biochemical information. These techniques are used to determine the histopathology of glial tumors¹⁷.

DWI and ADC maps, among these advanced MRI techniques, show tumor cellularity. The ADC values

obtained are inversely proportional to the tumor grade. Several studies have shown that ADC correlates well with tumor cellularity on histological examination. Calculation of ADC has been demonstrated that it can assist conventional MRI in characterizing glial tumors¹⁸. In our study, the detection rate of radiological grading with ADC values in addition to conventional MRI, mainly low-grade glial tumors, was higher than the radiological grading by conventional MRI.

Sugahara et al. published that the minimum ADC value correlated well with histological cellularity and was helpful in grading gliomas¹⁹. However, no significant difference between high-grade and low-grade glial tumors was observed in the studies of Rollin et al. and Lam et al.^{20,21}. Lee et al. elaborated that the average ADC values were 1.19 mm²/s and 1.035 mm²/s in high- and low-grade gliomas, respectively. Again, in this study, when the cutoff points were examined using the ROC analysis, the result was 1.055 mm²/s. Contrary to our findings, in significant ADC results between tumor grades could be due to the calculation made on a single section¹³. In our study, significant results were found only by taking diffusion-restricted regions from the tumor area.

Yamasaki et al. conducted measurements in astrocytic tumors and achieved a statistical accuracy of 91.3% between Grade II and high-grade (III and IV) tumors²². Server et al. also found a statistical difference between Grade II, Grade III, and Grade IV according to ADC values from tumor areas²³. In our study, considering the WHO grades in terms of ADC measurements, the difference between the groups was statistically significant. When the measurements were compared in pairs, the difference between Grades I and II, I and III, and I and IV. The difference between Grades II and III and II and IV was significant. Still, no significance was observed between Grades III and IV.

Advanced imaging techniques, such as MRS and PMRI, have been proposed in addition to ADC measurement to predict the grading of pre-operative brain gliomas²⁴. PMRI, which allows measurement of regional CBV (rCBV), shows a close correlation with the histopathological grade in gliomas²⁵. Schmainda et al. conducted a study on 73 patients with brain glioma and determined the rate of high- and low-grade glial tumors as 96% and 69%, respectively²⁶. In our study, when conventional and PMRI were evaluated, the detection rate of high- and low-grade glial tumors was 92.2% and 74.2%, respectively.

Studies conducted with PMRI in brain gliomas have shown that the rCBV cutoff point for distinguishing between high and low-grade glial tumors has not yet been determined²⁷. Yoon et al. reported the rCBV cutoff value as 2.44 in a study of 60 patients (12 low grade, 48 high grade), whereas Caulo et al. determined the cutoff value as 2.45 in 118 patients²⁸. In our study, the cutoff point was 1.77 (94% sensitivity and 64.5% specificity), similar to the results of Law et al. (1.75 in 120 high- and 40 low-grade glioma patients)⁹. Caulo et al. divided oligodendrogliomas and astrocytomas into degrees and found statistically significant differences between Grade III and Grade IV and Grade II and Grade III oligodendrogliomas. They also found a statistically significant difference between Grade II oligodendroglioma and Grade III astrocytoma²⁸. In our study, a significant difference was found only between Grade I and Grade IV and between Grades II and Grade IV, but no difference was found between other grades.

Studies on MRS elaborated that it is a powerful tool in brain tumor grading. Specifically, choline elevation with NAA depression is a reliable indicator in determining the character and metabolic status of the tumor²⁹. MRS provided additional information besides conventional MRI in the studies. In our study, when we compared the radiological grading through analyzing the metabolites in MRS in addition to conventional MRI with the pathological results, we recognized that the radiological grading was compatible with the pathological grading.

Law et al. found that Cho/Cr and Cho/NAA metabolite ratios were useful in determining tumor grade (97.5% and 96.7%, respectively)⁹. However, while high specificity was observed in identifying high-grade gliomas, lower specificity was observed in low-grade gliomas due to the smaller number of samples. In our study, in addition to conventional MRI, radiological grading was performed using Cho/NAA and Cho/Cr ratios one by one, and their superiority over each other was investigated. However, no significance was achieved.

Wang et al. conducted a meta-analysis conducted on 1228 patients and found that MRS was moderately successful in differentiating high-grade from low-grade gliomas. They also stated that the Cho/NAA ratio was superior to the NAA/Cr and Cho/Cr ratios in distinguishing high-grade gliomas from low-grade gliomas³⁰. Naveed et al. conducted a study with Grade II and Grade III oligodendrogliomas. They found that the Cho/NAA and Cho/Cr ratios were not statistically

different between the two groups³¹. In our study, we have also found that Cho/NAA and Cho/Cr were statistically significant.

Al-Okaili et al. performed a study with conventional MRI and advanced MRI techniques (DWI and ADC maps, MRS, and PMRI) on 111 patients through an algorithm with specific cutoff points. They distinguished high-grade glial tumors from low-grade ones with 90% accuracy and 88% sensitivity³². The results of glial tumor grading using the same algorithm in our study were that the detection rate of low-grade glial tumors was 83.9% and high-grade glial tumors 98%.

The limitation of our study is that glial tumors are rare tumors, so larger studies are needed. Furthermore, imaging methods are still insufficient to provide information about the molecular nature of the pathology. Therefore, imaging methods need to be improved. Furthermore, a comparison of this method with the normal population may give more support to the literature.

Conclusion

Using additional advanced MRI techniques such as PMRI, MRS, and DWI, with conventional MRI, could enhance the accuracy of histopathological grading in cranial glioma. A more consistent pre-operative WHO grading is possible when advanced MRI and cutoff points are considered in addition to conventional MRI findings.

Funding

The authors declare that they have not received funding.

Conflicts of interest

The authors declare no conflicts of interest.

Ethical disclosures

Protection of human and animal subjects. The authors declare that the procedures followed complied with the ethical standards of the responsible human experimentation committee and adhered to the World Medical Association and the Declaration of Helsinki. The procedures were approved by the institutional Ethics Committee.

Confidentiality, informed consent, and ethical approval. The authors have followed their institution's

confidentiality protocols, obtained informed consent from patients, and received approval from the ethics committee. The SAGER guidelines were followed according to the nature of the study.

Declaration on the use of artificial intelligence. The authors declare that no generative artificial intelligence was used in the writing of this manuscript.

References

1. Wang LM, Englander ZK, Miller ML, Bruce JN. Malignant glioma. *Adv Exp Med Biol.* 2023;1405:1-30.
2. Palacios-Saucedo GD, Padilla-Martínez JJ, Dávila-Gaytán AG, Herrera-Rivera CG, Vázquez-Guillén JM, Rivera-Morales LG, et al. Factores asociados a sobrevida a un año en pacientes postoperados de glioblastoma. *Cir Cir.* 2023;91:397-402.
3. Reuss DE. Updates on the WHO diagnosis of IDH-mutant glioma. *J Neurooncol.* 2023;162:461-9.
4. Moreno-Jiménez S, Martínez-Vaca N, Pérez-Aguilar B, Gómez-Calva B, Díaz-Chávez JJ, Mondragón-Soto MG. Usefulness and safety from stereotactic biopsy in posterior fossa lesions in adult patients. *Cir Cir.* 2019;87:554-8.
5. Hangel G, Schmitz-Abecassis B, Sollmann N, Pinto J, Arzanforoosh F, Barkhof F, et al. Advanced MR techniques for preoperative glioma characterization: part 2. *J Magn Reson Imaging.* 2023;57:1676-95. Erratum in: *J Magn Reson Imaging.* 2023.
6. Seo M, Choi Y, Soo Lee Y, Kim BS, Park JS, Jeon SS. Glioma grading using multiparametric MRI: head-to-head comparison among dynamic susceptibility contrast, dynamic contrast-enhancement, diffusion-weighted images, and MR spectroscopy. *Eur J Radiol.* 2023;165:110888.
7. Guarnera A, Romano A, Moltoni G, Ius T, Palizzi S, Romano A, et al. The role of advanced MRI sequences in the diagnosis and follow-up of adult brainstem gliomas: a neuroradiological review. *Tomography.* 2023;9:1526-37.
8. Sacli-Bilmez B, Danyelli AE, Yakicier MC, Aras FK, Pamir MN, Özduman K, et al. Magnetic resonance spectroscopic correlates of progression free and overall survival in "glioblastoma, IDH-wildtype, WHO grade-4". *Front Neurosci.* 2023;17:1149292.
9. Law M, Yang S, Wang H, Babb JS, Johnson G, Cha S, et al. Glioma grading: sensitivity, specificity, and predictive values of perfusion MR imaging and proton MR spectroscopic imaging compared with conventional MR imaging. *AJNR Am J Neuroradiol.* 2003;24:1989-98.
10. Arvinda HR, Kesavadas C, Sarma PS, Thomas B, Radhakrishnan VV, Gupta AK, et al. Glioma grading: sensitivity, specificity, positive and negative predictive values of diffusion and perfusion imaging. *J Neurooncol.* 2009;94:87-96. Retraction in: *J Neurooncol.* 2013;114:255.
11. Möller-Hartmann W, Herminghaus S, Krings T, Marquardt G, Lanfermann H, Pilatus U, et al. Clinical application of proton magnetic resonance spectroscopy in the diagnosis of intracranial mass lesions. *Neuroradiology.* 2002;44:371-81.
12. Kondziolka D, Lunsford LD, Martinez AJ. Unreliability of contemporary neurodiagnostic imaging in evaluating suspected adult supratentorial (low-grade) astrocytoma. *J Neurosurg.* 1993;79:533-6.
13. Lee EJ, Lee SK, Agid R, Bae JM, Keller A, Terbrugge K. Preoperative grading of presumptive low-grade astrocytomas on MR imaging: diagnostic value of minimum apparent diffusion coefficient. *AJNR Am J Neuroradiol.* 2008;29:1872-7.
14. Barker FG 2nd, Chang SM, Huhn SL, Davis RL, Gutin PH, McDermott MW, et al. Age and the risk of anaplasia in magnetic resonance-nonenhancing supratentorial cerebral tumors. *Cancer.* 1997;80:936-41.
15. Fan GG, Deng QL, Wu ZH, Guo QY. Usefulness of diffusion/perfusion-weighted MRI in patients with non-enhancing supratentorial brain gliomas: a valuable tool to predict tumour grading? *Br J Radiol.* 2006;79:652-8.
16. Dean BL, Drayer BP, Bird CR, Flom RA, Hodak JA, Coons SW, et al. Gliomas: classification with MR imaging. *Radiology.* 1990;174:411-5.
17. Su Y, Kang J, Lin X, She D, Guo W, Xing Z, et al. Whole-tumor histogram analysis of diffusion and perfusion metrics for noninvasive pediatric glioma grading. *Neuroradiology.* 2023;65:1063-71.
18. Ke X, Zhao J, Liu X, Zhou Q, Cheng W, Zhang P, et al. Apparent diffusion coefficient values effectively predict cell proliferation and determine oligodendroglioma grade. *Neurosurg Rev.* 2023;46:83.
19. Sugahara T, Korogi Y, Tomiguchi S, Shigematsu Y, Ikushima I, Kira T, et al. Posttherapeutic intraaxial brain tumor: the value of perfusion-sensitive contrast-enhanced MR imaging for differentiating tumor recurrence from nonneoplastic contrast-enhancing tissue. *AJNR Am J Neuroradiol.* 2000;21:901-9.
20. Rollin N, Guyotat J, Streichenberger N, Honnorat J, Tran Minh VA, Cotton F. Clinical relevance of diffusion and perfusion magnetic resonance imaging in assessing intra-axial brain tumors. *Neuroradiology.* 2006;48:150-9.

21. Lam WW, Poon WS, Metreweli C. Diffusion MR imaging in glioma: does it have any role in the pre-operation determination of grading of glioma? *Clin Radiol.* 2002;57:219-25.
22. Yamasaki F, Kurisu K, Satoh K, Arita K, Sugiyama K, Ohtaki M, et al. Apparent diffusion coefficient of human brain tumors at MR imaging. *Radiology.* 2005;235:985-91.
23. Server A, Kulle B, Gadmar ØB, Josefsen R, Kumar T, Nakstad PH. Measurements of diagnostic examination performance using quantitative apparent diffusion coefficient and proton MR spectroscopic imaging in the preoperative evaluation of tumor grade in cerebral gliomas. *Eur J Radiol.* 2011;80:462-70.
24. Su X, Yang X, Sun H, Liu Y, Chen N, Li S, et al. Evaluation of key molecular markers in adult diffuse gliomas based on a novel combination of diffusion and perfusion MRI and MR spectroscopy. *J Magn Reson Imaging.* 2024;59(2):628-638.
25. Amjad G, Zeinali Zadeh M, Azmoudeh-Ardalan F, Jalali AH, Shakiba M, Ghavami N, et al. Evaluation of multimodal MR imaging for differentiating infiltrative versus reactive edema in brain gliomas. *Br J Neurosurg.* 2023;37:1031-9.
26. Schmainda KM, Rand SD, Joseph AM, Lund R, Ward BD, Pathak AP, et al. Characterization of a first-pass gradient-echo spin-echo method to predict brain tumor grade and angiogenesis. *AJNR Am J Neuroradiol.* 2004;25:1524-32.
27. Sanvito F, Raymond C, Cho NS, Yao J, Hagiwara A, Orpilla J, et al. Simultaneous quantification of perfusion, permeability, and leakage effects in brain gliomas using dynamic spin-and-gradient-echo echoplanar imaging MRI. *Eur Radiol.* 2024;34(5):3087-3101.
28. Caulo M, Panara V, Tortora D, Mattei PA, Briganti C, Pravatà E, et al. Data-driven grading of brain gliomas: a multiparametric MR imaging study. *Radiology.* 2014;272:494-503.
29. Ankush A, Sardesai S. Role of MRSI major metabolite ratios in differentiating between intracerebral ring-enhancing neoplastic and non-neoplastic lesions, high-grade gliomas and metastases, and high-grade and low-grade gliomas. *Cureus.* 2022;14:e31841.
30. Wang Q, Zhang H, Zhang J, Wu C, Zhu W, Li F, et al. The diagnostic performance of magnetic resonance spectroscopy in differentiating high-from low-grade gliomas: a systematic review and meta-analysis. *Eur Radiol.* 2016;26:2670-84.
31. Naveed MA, Goyal P, Malhotra A, Liu X, Gupta S, Mangla M, et al. Grading of oligodendroglial tumors of the brain with apparent diffusion coefficient, magnetic resonance spectroscopy, and dynamic susceptibility contrast imaging. *Neuroradiol J.* 2018;31:379-85.
32. Al-Okaili RN, Krejza J, Wang S, Woo JH, Melhem ER. Advanced MR imaging techniques in the diagnosis of intraaxial brain tumors in adults. *Radiographics.* 2006;26 Suppl 1:S173-89.